Acta Pharmacologica Sinica 2017: 1269–1281
 1671-4083/17
www.nature.com/aps

Original Article

The novel α-glucan YCP improves the survival rates and symptoms in septic mice by regulating myeloid-derived suppressor cells

Dan LIU[1, 4], Ming YOU[1], Guang-feng ZHAO[4], Xiu-jun LI[1], Yu-xian SONG[1, 5], Huan DOU[1, 3], Wen-bing YAO[2], Xiang-dong GAO[2, *], Ya-yi HOU[1, 3, *]

[1]The State Key Laboratory of Pharmaceutical Biotechnology, Division of Immunology, Medical School, Nanjing University, Nanjing 210093, China; [2]The State Key Laboratory of Natural Medicines, School of Life Science and Technology, China Pharmaceutical University, Nanjing 210009, China; [3]Jiangsu Key Laboratory of Molecular Medicine, Nanjing 210093, China; [4]The Affiliated Drum Tower Hospital of Nanjing University Medical School, Nanjing 210093, China; [5]Central Laboratory of Stomatology, Nanjing Stomatology Hospital and the State Key Laboratory of Pharmaceutical Biotechnology, Division of Immunology, Medical School, Nanjing University, Nanjing 210093, China

Abstract

Sepsis is a life-threatening health condition that is initially characterized by uncontrolled inflammation, followed by the development of persistent immunosuppression. YCP is a novel α-glucan purified from the mycelium of the marine fungus *Phoma herbarum* YS4108, which has displayed strong antitumor activity via enhancing host immune responses. In this study, we investigated whether YCP could influence the development of sepsis in a mouse model. Caecal ligation and puncture (CLP)-induced sepsis was established in mice that were treated with YCP (20 mg/kg, ip or iv) 2 h before, 4 and 24 h after the CLP procedure, and then every other day. YCP administration greatly improved the survival rate (from 39% to 72% on d 10 post-CLP) and ameliorated disease symptoms in the septic mice. Furthermore, YCP administration significantly decreased the percentage of myeloid-derived suppressor cells (MDSCs) in the lungs and livers, which were dramatically elevated during sepsis. In cultured BM-derived cells, addition of YCP (30, 100 μg/mL) significantly decreased the expansion of MDSCs; YCP dose-dependently decreased the phosphorylation of STAT3 and increased the expression of interferon regulatory factor-8 (IRF-8). When BM-derived MDSCs were co-cultured with T cells, YCP dose-dependently increased the production of arginase-1 (Arg-1) and inducible nitric oxide synthase (iNOS), and activated the NF-κB pathway. In addition, the effects of YCP on MDSCs appeared to be dependent on toll-like receptor (TLR) 4. These results reveal that YCP inhibits the expansion of MDSCs via STAT3 while enhancing their immunosuppressive function, partially through NF-κB. Our findings suggest that YCP protects mice against sepsis by regulating MDSCs. Thus, YCP may be a potential therapeutic agent for sepsis.

Keywords: YCP; α-glucan; sepsis; myeloid-derived suppressor cells; STAT3; IRF-8; arginase-1; iNOS; NF-κB; TLR4

Acta Pharmacologica Sinica (2017) 38: 1269–1281; doi: 10.1038/aps.2017.27; published online 26 Jun 2017

Introduction

Sepsis is defined as a host inflammatory response to a life-threatening infection with the presence of some degree of organ dysfunction[1, 2]. It is an increasingly common and lethal medical condition that occurs in people of all ages. It is the leading cause of mortality in intensive care units (ICUs) worldwide[3-5]. Therefore, new drug development and more effective therapies targeting sepsis are in high demand. Recent studies have demonstrated that both overwhelming pro-inflammatory and anti-inflammatory responses occur rapidly and simultaneously during sepsis. Although unrestrained inflammation is dominant in the early phase[3, 6–8], this initial hyper-inflammatory response evolves into a prolonged immunosuppressive stage several days later[9, 10]. Several studies have suggested that sepsis-associated immunosuppression increases mortality; hence, therapies that balance pro- and anti-inflammatory pathways may be effective strategies for improving the survival rate of septic patients[3, 9].

Various natural polysaccharides possess the ability to activate the immune system. It has been reported that β-glucan and α-glucan protect against both infections[11–14] and malignancies[12]. We have previously identified a novel α-glucan with a molecular weight of 2.4×10^3 kDa, which we purified

*To whom correspondence should be addressed.
E-mail yayihou@nju.edu.cn (Ya-yi HOU);
xdgao@cpu.edu.cn (Xiang-dong GAO)
Received 2016-10-11 Accepted 2017-02-04

from the mycelium of the marine fungus *Phoma herbarum* YS4108, named YCP. YCP exhibits strong antitumor activity by enhancing the host's immunity[15–18]. YCP treatment induces nitric oxide (NO) production in macrophages[16], promotes the proliferation of murine splenic B cells[17, 18], provides a second signal for T cells and effectively stimulates dendritic cells (DCs) to secrete interleukin (IL)-12 and express surface activation markers[15]. Moreover, we have found that toll-like receptor (TLR) 4 may be responsible for the functions of YCP[15–18]. However, it remains unclear whether YCP can influence the development of sepsis.

Sepsis deeply perturbs immune homeostasis[8] and directly or indirectly affects almost all types of immune cells[3]. Recent studies have shown that the development of sepsis is related to the expansion of myeloid-derived suppressor cells (MDSCs)[19–23]. MDSCs, which are a heterogeneous population of immature myeloid cells composed of following two subsets, monocytic MDSCs (M-MDSCs) and granulocytic MDSCs (G-MDSCs), are a major component of the immunosuppressive network in many pathological conditions, including sepsis[24–26]. MDSCs are dramatically increased in lung tissues[27] and blood samples[22, 28] obtained from sepsis patients. Moreover, in the cecal ligation and puncture (CLP)-induced model of sepsis in mice, the number of MDSCs gradually increases and remains dramatically elevated in the bone marrow (BM), spleen, blood, and lymph nodes[19, 21, 29, 30]. Notably, MDSCs may evolve during the development of sepsis[21, 29, 31]. It has been found that the adoptive transfer of MDSCs harvested at the late stage of sepsis into naive mice immediately after CLP surgery decreases pro-inflammatory cytokine production, increases peritoneal bacterial growth, and improves survival rate[21, 29]. In addition, *in vitro* experiments have shown that these MDSCs are highly responsive to lipopolysaccharide (LPS) in terms of cytokine secretion, NF-kB activation, reactive oxygen species (ROS) production and arginase I (Arg-1) activity[21]. Conversely, MDSCs obtained from early stage sepsis promote the opposite effects[21, 29]. These observations strongly suggest that the heterogeneous MDSCs might shift their state as the sepsis inflammatory process progresses[29]. Furthermore, recent findings have also suggested that MDSCs may be amenable targets for host-directed therapies[26, 32]. Hence, a better understanding of MDSC generation and/or regulation may provide novel insights for the treatment of sepsis.

In the present study, we aimed to investigate the potentially protective effect of the α-glucan YCP against CLP-induced sepsis in mice and the possible underlying mechanisms. Our results showed that YCP significantly improved the survival rates of the septic mice and resulted in a decreased percentage of MDSCs. Therefore, we further explored how YCP regulates MDSCs. Our findings provide evidence for the potential use of YCP in the treatment of sepsis.

Materials and methods

Materials

YCP is a natural α-glucan with a molecular weight (M_W) of 2.4×10^3 kDa. YCP was purified from the mycelium of the marine filamentous fungus *Phoma herbarum* YS4108, which inhabits the sediment in the Yellow Sea area near Yancheng, China. YCP has a backbone of α-1,4-*D*-glucans with a lower proportion of α-1,6-linked glucopyranosyl and glucuronic acid residues as non-reducing termini. YCP was purified by a combination of ion-exchange chromatography on DEAE-32 and gel permeation over Sephacryl S-400[33]. The purity of YCP was shown as a single chromatographic peak on an Agilent 1100 HPLC system equipped with a gel permeation chromatographic column Shodex KS-805. The endotoxin contamination in YCP was also proven to be negligible by an LAL chromogenic endpoint assay[17].

Animals

C57BL/6J male mice (8–12 weeks old, 25–30 g) were purchased from the Animal Model Research Institute of Nanjing University (Nanjing, China). The mice were then housed in a pathogen-free barrier facility under a 12 h light/dark cycle. The experimental methods described here were carried out in accordance with the guidelines of the Experimental Animal Management Committee (Jiangsu Province, China). All procedures were approved by the Committee on the Ethics of Animal Experiments at Nanjing University (SYXK 2014-0052).

Cell culture

BM-derived MDSCs were obtained as previously described[34]. In brief, BM cells were flushed from the femurs and tibias of approximately 10-week-old C57BL/6J mice. The red blood cells (RBCs) were lysed with an ACK lysis buffer containing 0.15 mol/L NH_4Cl, 10 mmol/L $KHCO_3$, and 0.1 mmol/L Na_2EDTA. The BM cells were then cultured in an RPMI-1640 medium supplemented with 10% FBS (Gibco/Invitrogen Corporation, CA, USA), 100 U/mL penicillin and 100 U/mL streptomycin and stimulated with 40 ng/mL IL-6 (PeproTech, Rocky Hill, NJ, USA) and granulocyte-macrophage colony-stimulating factor (GM-CSF) (Miltenyi Biotec, Bergisch Gladbach, Germany) at 37°C in a 5% CO_2-humidified atmosphere for 4 d. For the MDSC expansion experiments, the culture medium was additionally supplemented with varying concentrations of YCP.

Cecal ligation and puncture model of sepsis

CLP was performed as previously described[35]. In this study, we ligated the cecum halfway between the distal pole and the base and perforated the cecum with a single puncture midway between the ligation and the cecum tip. The control sham-operated mice were treated identically except for that the cecum was neither ligated nor punctured. CLP mice were randomly assigned to groups receiving injections of either YCP or sterile saline. In the YCP-treated group, mice received 20 mg/kg YCP dissolved in saline by intraperitoneal injections 2 h before, 4 h after and 24 h after the CLP procedure and every other day after that. In both the sham-operated and CLP groups, control mice received sterile saline. After the experiment, all mice were euthanized, and tissue samples were collected. To test the effect of YCP on the survival rate of

the septic mice, YCP was administered both intraperitoneally and intravenously.

Blood and peritoneal bacterial culture

Blood and peritoneal lavage fluid were collected from the mice immediately after euthanasia and were then serially diluted with sterile saline. The blood was plated in 5% sheep blood agar plates, and the peritoneal lavage fluid was plated in agar plates. All plates were incubated for 18 h at 37 °C under aerobic conditions. CFUs were counted and multiplied by the dilution factor for the bacterial load quantification. The results are expressed as CFU counts per milliliter of blood or peritoneal lavage fluid.

Cytokine measurements

The sera and bronchoalveolar lavage fluid (BALF) samples were collected 24 h after the CLP operation. To obtain the sera, blood was collected and centrifuged at 900×*g* for 10 min; after the coagulation at room temperature, the sera were separated and stored at -80 °C. To obtain BALF, 20 μL of 1× PBS per gram of mouse body weight was injected and retrieved following tracheostomy. The BALF was centrifuged at 900×*g* for 10 min at 4 °C, and the supernatants were stored at -80 °C until use in the cytokine expression analysis. The levels of IL-6 and tumor necrosis factor-α (TNFα) in serum and BALF were measured with enzyme-linked immunosorbent assays (ELISA) (BioLegend, San Diego, CA, USA).

Reverse transcription PCR and quantitative real-time PCR analysis

The total RNA of the BM-derived MDSCs was extracted with the TRIzol reagent (Invitrogen, San Diego, CA, USA) according to the manufacturer's instructions. Following the extraction, oligo(dT) primers were used to reverse-transcribe the mRNA into cDNA. Quantitative real-time PCR (q-PCR) assays were performed on a StepOne Plus or an ABI Vii 7 detection system (Applied Biosystems, Foster City, CA, USA) with SYBR Green PCR master mix solution. The relative gene expression was calculated with the $2^{-\Delta CT}$ formula; GAPDH was used as the internal control.

Flow cytometry analysis

To obtain single cell suspensions, the lung and liver tissues were cut into small pieces and digested in RPMI-1640 containing 3 mg/mL collagenase I or IV at 37 °C for 30 min on a shaker. The BM cells were flushed from the femurs and tibias. The spleens were mashed to obtain the splenocytes. The cells derived from each tissue sample were separately passed through a 200-mesh sieve. The RBCs were removed by ACK lysis. MDSCs were labeled with CD11b-APC and Gr1-PE. The M-MDSCs and G-MDSCs were uniquely detected by CD11b-FITC, Ly6G-APC (clone: 1A8), and Ly6C-PE. All antibodies and isotype-matched controls were purchased from BD Pharmingen™ (San Diego, CA, USA). The appropriate isotype-matched control was used for each antibody. The BM cells, which were treated with YCP at concentrations of 0, 10, 30 or 100 μg/mL for 2 d, were stained with Annexin V and PI to detect apoptotic cells using the Annexin V-FITC & PI Apoptosis Kit (Biouniquer, San Diego, CA, USA). The BM-derived MDSCs were harvested and incubated with DCFH-DA (Beyotime, Shanghai, China) to measure the levels of ROS. Flow cytometry was performed on a FACSCalibur flow cytometer (Becton Dickinson, Franklin Lakes, NJ, USA). The data were analyzed using FlowJo software (Treestar, Inc, San Carlos, CA, USA).

Western blotting

Western blotting was performed as described previously[36]. Anti-mouse p-STAT3 (Cell Signaling Technology (CST), Danvers, MA, USA), STAT3 (CST), anti-arginine (Bioworld, MN, USA), anti-p-p65 (CST), and anti-GAPDH (CST) were used as primary antibodies. Horseradish peroxidase (HRP)-conjugated goat anti-rabbit or anti-mouse antibodies were used as secondary antibodies. The Immobilon Western Chemiluminescent HRP Substrate (Millipore, Billerica, MA, USA) was used to detect the protein bands. Images were obtained using the MiniChemi™ Chemiluminescence imaging system (Sage Creation, Beijing, China).

Cell viability assays

The cytotoxicity of YCP on BM cells was measured by a Cell Counting Kit-8 (CCK-8; Dojindo, Kumamoto, Japan) according to the manufacturer's protocol. The BM cells were treated with different concentrations of YCP in the presence of IL-6 and GM-CSF (40 ng/mL). Two or four days later, the cell viability was measured.

MDSC sorting and T cell proliferation

To obtain high-purity MDSCs, an MDSC isolation kit (Miltenyi Biotec) was used according to the manufacturer's instructions. For the T cell suppression assay, all splenic T cells were isolated from the C57BL/6J mice via negative selection using a mouse-Pan T cell isolation kit II (Miltenyi Biotec) and activated with anti-CD3 and anti-CD28 antibodies. The BM-derived MDSCs were treated with 50 μg/mL YCP or 1× PBS during their differentiation process *in vitro*. YCP was then removed, and high-purity G-MDSCs ($Gr1^{high}Ly6G^{+}$) and M-MDSCs ($Gr1^{dim}Ly6G^{-}$) were isolated. G-MDSCs were co-cultured at 1:1, 1:2, or 1:4 ratios with T cells, and M-MDSCs were co-cultured at 1:2 or 1:4 ratios with T cells in 96-well flat-bottom plates. T-cell proliferation was assessed by [^{3}H]thymidine incorporation 72 h later.

Nitrite and arginase assays

BM-derived MDSCs cultured with 10 ng/mL IL-6 and GM-CSF were treated with YCP at concentrations of 0, 10, 30 or 100 μg/mL for 24 h. NO production was measured in the culture supernatants using the Griess reagent according to the manufacturer's protocol. To assess arginase activity, BM-derived MDSCs were harvested after the treatment with YCP for 36 h, and the activity was measured in the cell lysate with an arginase assay kit (BioAssay Systems, Hayward, CA,

USA). In brief, approximately 1×10^6 cells were harvested and lysed in 100 μL of 10 mmol/L Tris-HCl (pH 7.4) containing 1 μmol/L pepstatin A, 1 μmol/L leupeptin, and 0.4% (*w*/*v*) Triton X-100 for 10 min. The lysates were centrifuged at 14 000×*g* for 10 min, and the supernatants were collected for the arginase activity assessment. All samples were diluted 5 times, and then, 40 μL of the diluted samples were mixed with 10 μL of the 5× substrate buffers in a 96-well plate, which was incubated at 37 °C for 2 h. The reaction was stopped by adding 200 μL of the supplied urea reagent to all wells. The plate was incubated for 60 min at room temperature, and the optical density was read at 430 nm. Arginase activity was calculated according to the formula provided by the manufacturer.

Statistical analysis

All data were analyzed with Prism 5 (GraphPad Software, Inc, San Diego, CA, USA) and expressed as the mean±SEM. Student's *t*-tests (two-tailed) were used to compare the differences between the various treatment groups. Statistical comparisons between the survival curves were performed using a log-rank (Mantel-Cox) test. Differences with $P<0.05$ were considered statistically significant. The *in vitro* experiments were repeated independently at least three times.

Results

YCP improves survival and ameliorates disease symptoms in septic mice

To study the effect of YCP on CLP-induced polymicrobial sepsis, mice were treated with YCP several times before and after the CLP surgery. Intriguingly, we found that YCP significantly improved the survival rates of the septic mice regardless of whether it was administered through intraperitoneal or intravenous injections. After the study (10 d post-CLP), the survival rates had increased to 72% in the group treated with YCP intraperitoneally compared with only 39% in the control CLP group (Figure 1A). The intravenous administration of YCP also increased the survival rate from 36% to 71% (Figure 1A).

To elucidate the effects of YCP during sepsis, we evaluated the disease symptoms in septic mice with or without the YCP treatment. We found that the YCP treatment reduced the bacterial colony forming unit (CFU) counts in both the blood and peritoneal fluid (Figure 1B), which were collected 24 h after the CLP procedure. The YCP treatment also significantly reduced the levels of the inflammatory cytokines IL-6 and TNFα in the sera (Figure 1C) and the level of IL-6 in the bronchoalveolar lavage fluid (BALF) samples collected from the septic mice (Figure 1D). Additionally, the levels of the biochemical indicators of organ function were assessed in the sera. The aspartate aminotransferase (AST), alanine aminotransferase (ALT), and blood urea nitrogen (BUN) levels were all increased in the septic mice compared with those in the sham-operated mice, whereas the creatinine levels remained unchanged (Figure 1E). The YCP treatment decreased the systemic levels of AST and BUN but did not affect the levels of ALT and creatinine (Figure 1E). Furthermore, a histological assessment of lung, liver and kidney sections stained with hematoxylin and eosin also revealed multiple organ damage. The organ specimens from the CLP group displayed histological abnormalities and marked inflammatory infiltration. The specimens from the YCP-treated mice showed a substantial suppression of CLP-induced pathology in terms of both damage and inflammatory infiltration (Figure 1F). Altogether, these data demonstrate that the YCP treatment can effectively improve survival and ameliorate disease symptoms in septic mice.

YCP reduces the percentage of MDSCs in the lungs and livers of septic mice

Recent studies have demonstrated that the number of MDSCs dramatically increases and remains elevated in the BM, spleen, blood, and lymph nodes of CLP-induced septic mice[19, 21, 29, 30]. In this study, our results showed that the percentage of $CD11b^+Gr1^+$ MDSCs was not only significantly increased in the BM and spleen but was also elevated in the damaged lungs and livers of the mice that underwent CLP (Figure 2A, 2B).

Interestingly, we found that the YCP treatment appeared to decrease the frequency of MDSCs in both the lung and liver but not in the BM or spleen (Figure 2A, 2B). Despite this effect, the YCP treatment did not change the percentage of macrophages in either the lung or liver (Figure 2C). These observations were further confirmed by immunofluorescence assays (Figure 2D). Surprisingly, YCP preferentially decreased the percentage of G-MDSCs ($CD11b^+Ly6G^+Ly6C^{low}$) even though both G-MDSCs and M-MDSCs ($CD11b^+Ly6G^-Ly6C^{high}$) were increased in the septic mice (Figure 2E). These results suggest that YCP may protect the septic mice by decreasing the accumulation of MDSCs.

YCP inhibits the expansion of MDSCs *in vitro* via a STAT3-dependent pathway

The effect of YCP on mouse BM cells was first detected *in vitro*. Our results showed that low concentrations of YCP did not promote cytotoxicity in BM cells even after being co-cultured for up to 4 d (Figure 3A). Therefore, concentrations less than or equal to 100 μg/mL were chosen for the following *in vitro* experiments. However, YCP did decrease the number of BM cells (Figure 3B), which was attributed to BM cell apoptosis *in vitro* (Figure 3C, 3D).

To investigate the effect of YCP on the expansion of MDSCs, mouse BM cells were induced to differentiate into MDSCs. During the MDSC differentiation, varying concentrations of YCP were added to the culture medium, and a 1× PBS treatment was used as the control. We found that YCP significantly inhibited the expansion of MDSCs at d 2 and d 4 (Figure 4A, 4B). Notably, the YCP treatment significantly decreased G-MDSCs in a concentration-dependent manner, whereas M-MDSCs were decreased only when treated with high concentrations (Figure 4C, 4D), which is in agreement with the *in vivo* results.

Previous reports have shown that signal transducer and activator of transcription 3 (STAT3) is the main transcription factor that regulates the expansion of MDSCs under pathologi-

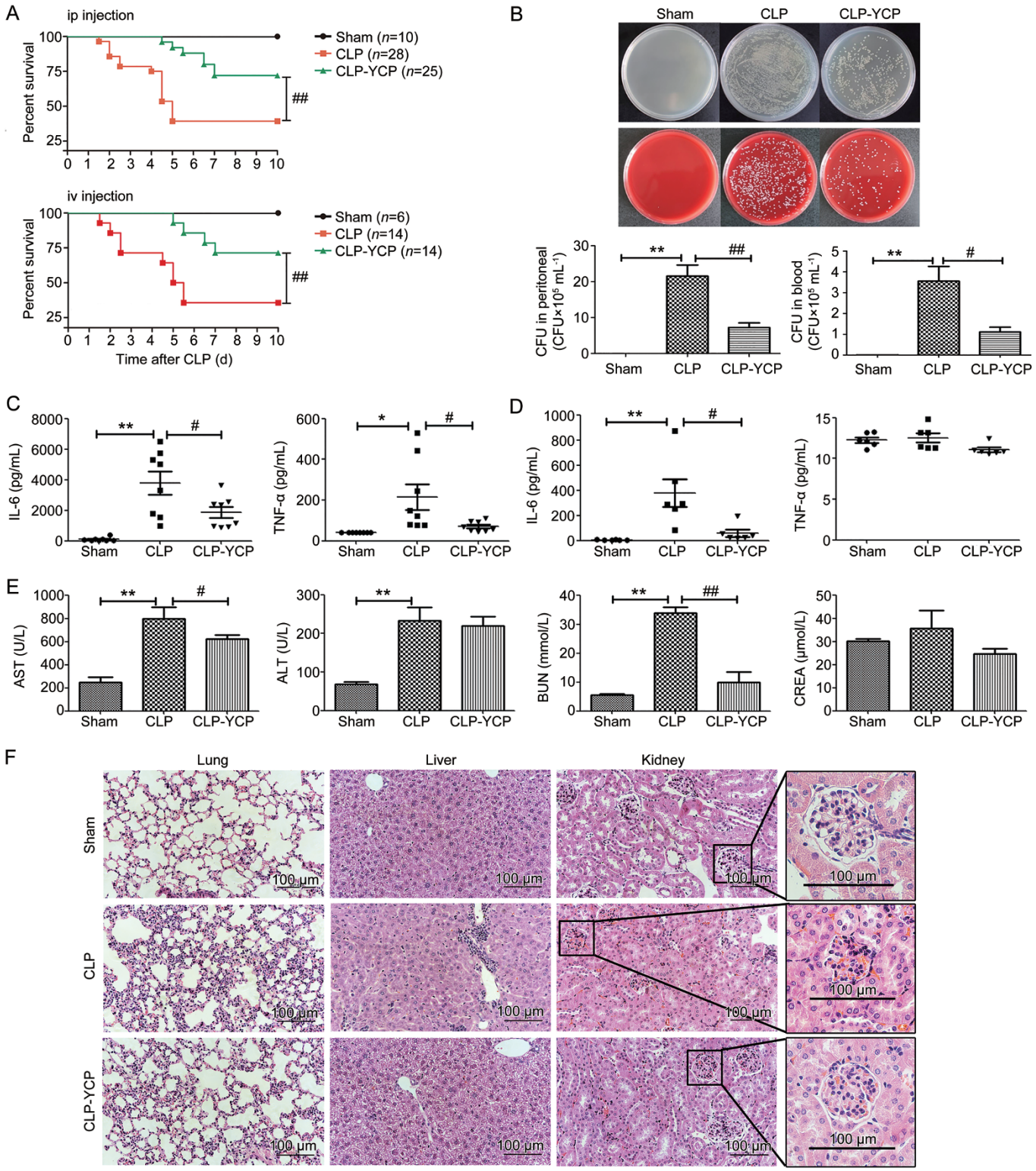

Figure 1. YCP improves survival and ameliorates disease symptoms in septic mice. (A) The survival rates of CLP-induced septic mice and sham-operated mice were monitored for 10 d. Septic mice were treated with YCP via intraperitoneal (ip) or intravenous (iv) injections. The control septic mice group and the sham-operated mice were treated with saline. (B–E) In a separate experiment (n=8 per group), the mice were euthanized 24 h after CLP. (B) The number of CFUs in the blood and peritoneal fluid was quantified. The levels of IL-6 and TNFα in sera (C) or BALF samples (D) were measured by ELISA, and the levels of AST, ALT, BUN, and CREA were detected. (F) In this experiment, the lung, liver, and kidney tissues of all mice (n≥5 per group) that survived for 5 d were fixed and subjected to H&E staining. Representative images are presented. (A) Statistical comparisons were performed using a log-rank (Mantel-Cox) test. (B-E) Values represent the mean±SEM of mice in each group, and all data were analyzed with Student's t-test. $^{*}P$<0.05, $^{**}P$<0.01, sham-operated versus CLP group. $^{\#}P$<0.05, $^{\#\#}P$<0.01, CLP versus YCP-treated group.

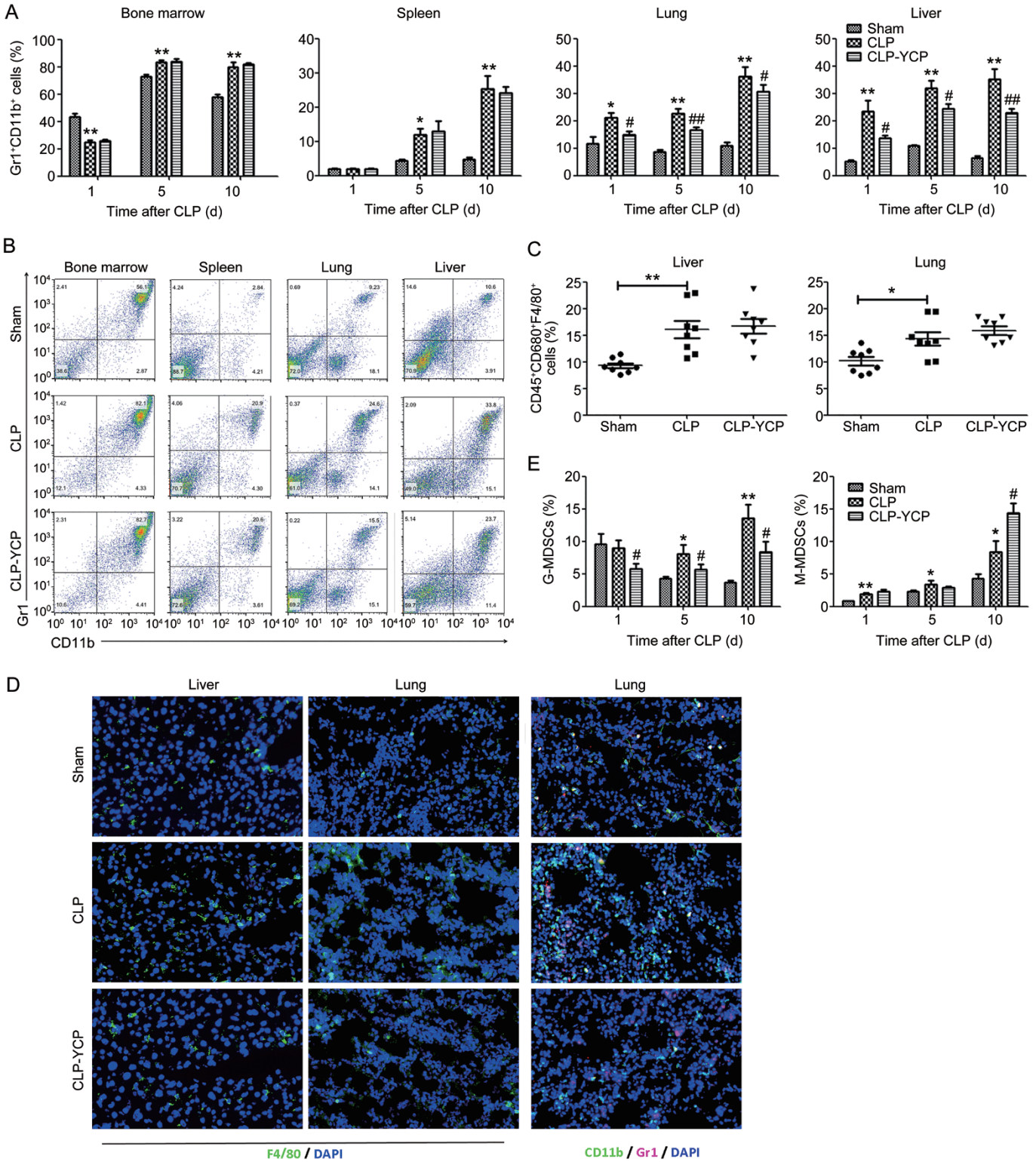

Figure 2. YCP reduces the accumulation of MDSCs in the lungs and livers of mice that survived sepsis. (A) The percentages of $Gr1^+CD11b^+$ MDSCs in the BM, spleen, lungs, and livers of mice that were treated with or without YCP and survived at 1 d, 5 d and 10 d after the CLP surgery ($n \geq 5$ per group). (B) Representative flow cytometry dot plot of cells isolated from different tissues of mice and stained with Gr1-PE and CD11b-APC. (C) The percentage of macrophages identified by $CD45^+CD68^+F4/80^+$ staining in the lung and liver tissues of mice surviving for 24 h post-CLP. (D) Frozen sections of lung and liver tissues obtained 24 h after CLP stained with anti-F4/80 (Abcam) or anti-Gr1-594 (BioLegend) and anti-CD11b-FITC. DAPI was used to stain the cell nuclei. All images were taken under the same 10× objective. (E) The percentage of G-MDSCs ($CD11b^+Ly6G^+Ly6C^{low}$) and M-MDSCs ($CD11b^+Ly6G^-Ly6C^{high}$) in the lungs of mice ($n \geq 5$ per group). The values represent the mean±SEM of 5-10 mice per group, and all data were analyzed with Student's *t*-test. $^*P<0.05$, $^{**}P<0.01$, sham-operated versus CLP group. $^{\#}P<0.05$, $^{\#\#}P<0.01$, CLP versus YCP-treated group.

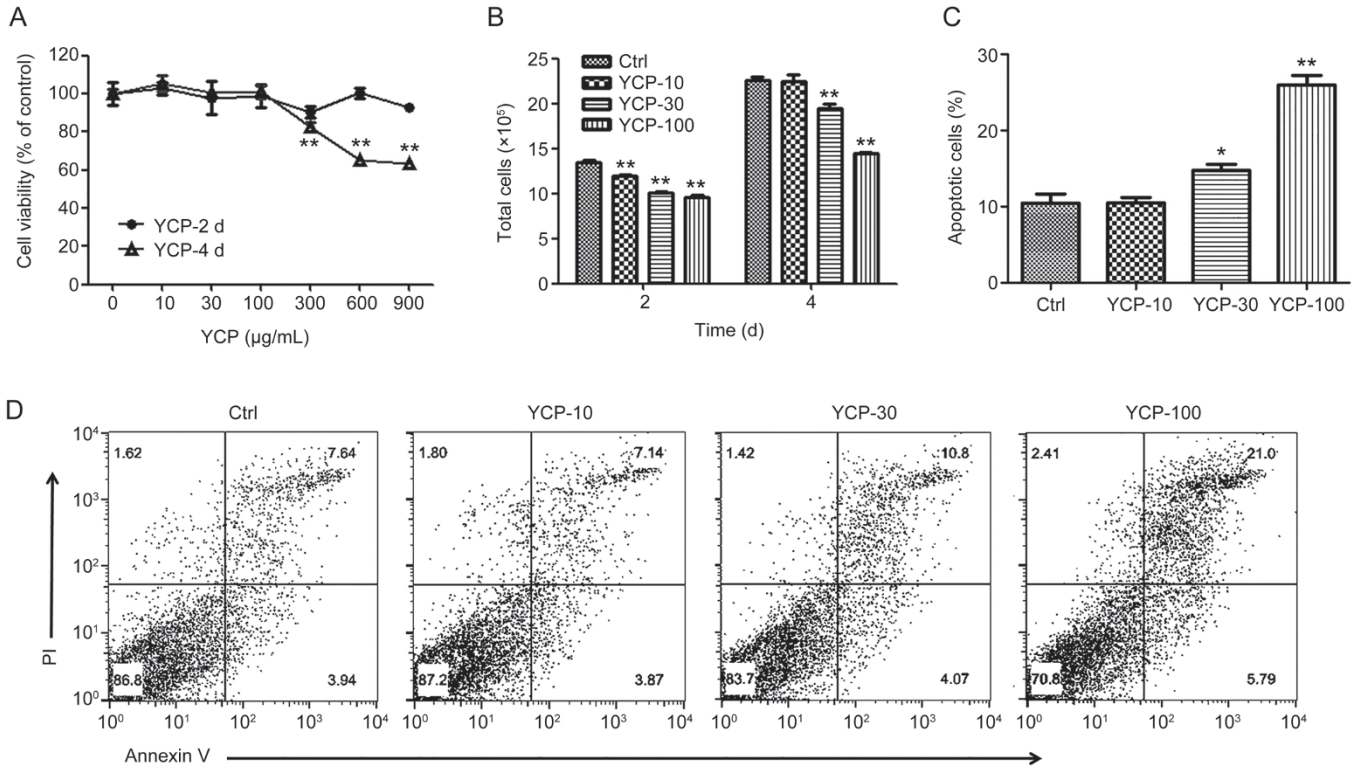

Figure 3. YCP promotes the apoptosis of BM-derived cells *in vitro*. To explore the effect of the YCP treatment on MDSCs *in vitro*, BM cells were obtained and cultured with 40 ng/mL IL-6 and GM-CSF, which induced the differentiation of BM cells into MDSCs. (A) Varying concentrations of YCP were applied to the BM cells to assess YCP-related cytotoxicity, and CCK8 assays were used to measure the cell viability. (B) Equal numbers of BM cells were treated with varying concentrations of YCP for 2 or 4 d; then, the cell numbers were counted. (C, D) The effect of YCP on the apoptosis of BM cells was measured by flow cytometry. BM cells were treated with YCP for 2 d and then stained with PI and Annexin V. The values represent the mean±SEM, and all data were analyzed with Student's *t*-test. The experiments were repeated independently three times. $^{*}P<0.05$, $^{**}P<0.01$, compared to the corresponding controls.

cal conditions. Abnormal and persistent activation of STAT3 in myeloid progenitor cells promotes MDSC expansion[37–39]. Moreover, the expression of interferon regulatory factor-8 (IRF-8), which is downstream of STAT3, negatively regulates the accumulation of MDSCs in a STAT3-dependent manner[40]. STAT3 also regulates the expansion of MDSCs by inducing S100 calcium-binding protein A8 (S100A8) and S100A9 expression[41, 42]. In our study, we found that YCP significantly reduced the phosphorylation of STAT3 (Figure 4E) and induced the expression of IRF-8 (Figure 4F). Additionally, our results showed that YCP repressed the expression of S100A8 and S100A9 (Figure 4G). Altogether, these data strongly suggest that YCP inhibits the expansion of MDSCs through a STAT3-dependent pathway.

YCP enhances the function of MDSCs partially through the NF-κB pathway

To investigate the function of MDSCs, we co-cultured BM-derived MDSCs with T cells. Surprisingly, we found that the YCP treatment enhanced the immunosuppressive function of both G-MDSCs and M-MDSCs toward T cells (Figure 5A). The levels of Arg-1, inducible nitric oxide synthase (iNOS) and ROS are essential for MDSC-mediated immunosuppression[19, 20, 37, 43, 44] under certain pathological conditions. Thus, we explored whether YCP exerted its function through these molecules. The results demonstrated that YCP promoted the production of iNOS (Figure 5B, 5C) and Arg-1 (Figure 5D–5F), but not ROS (Figure 5G), in the BM-derived MDSCs. Our previous studies have shown that YCP activates the NF-κB pathway in macrophages[16] and B cells[17]. In this study, our results also showed that YCP activated the NF-κB pathway in MDSCs (Figure 5H). Furthermore, we detected the expression levels of iNOS, Arg-1, $P47^{phox}$ and $gp91^{phox}$ in MDSCs isolated from the spleens of septic mice that survived 3 d after the CLP operation and were treated with or without YCP. In addition, we found that the YCP treatment promoted the expression of iNOS and Arg-1 but did not affect the expression of $P47^{phox}$ and $gp91^{phox}$ (Figure 5I), which were relative to the production of ROS, *in vivo*. In addition, these results were consistent with the *in vitro* results. Thus, our results indicate that YCP enhances the immunosuppressive function of MDSCs, at least partially, through the NF-κB pathway.

TLR4 acts as the YCP receptor on MDSCs

We have previously found that YCP binds to cells through an interaction with TLR2 and TLR4[15–18]. To determine whether

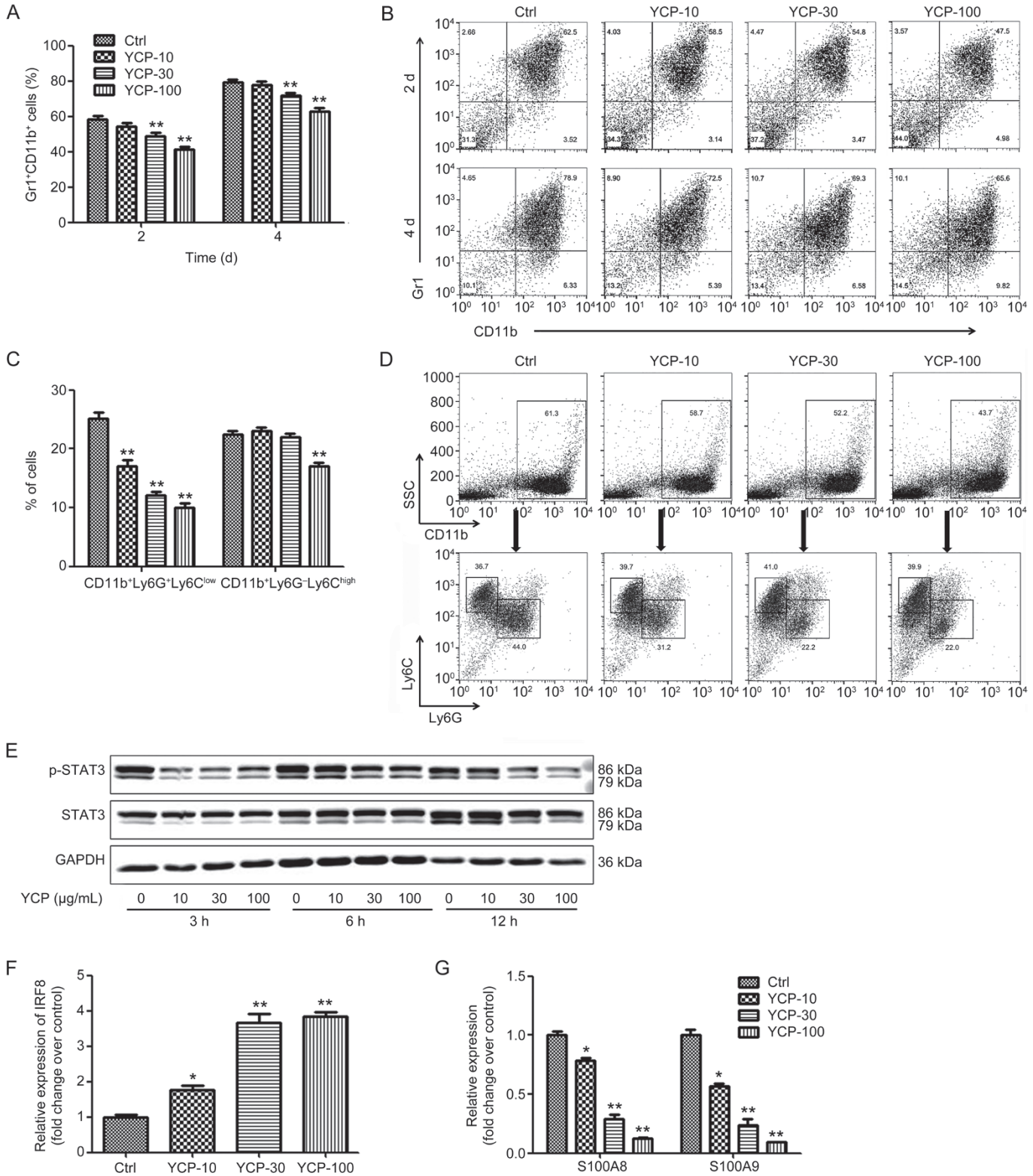

Figure 4. YCP inhibits the expansion of MDSCs via a STAT3-dependent pathway *in vitro*. BM cells were cultured with 40 ng/mL IL-6 and GM-CSF and treated with YCP. (A, B) The percentage of BM-derived MDSCs ($Gr1^+CD11b^+$) was measured by flow cytometry at d 2 and d 4. (C) The percentages of G-MDSCs and M-MDSCs were detected by anti-CD11b, anti-Ly6G and anti-Ly6C and measured by flow cytometry at d 2 and d 4. (D) Representative flow cytometry dot plots obtained at d 2. (E) Protein extracted from BM cells treated with YCP for 3 h, 6 h or 12 h was collected, and p-STAT3 and total-STAT3 were detected by Western blotting. The images are from different parts of the same gel. Q-PCR was used to detect the expression levels of IRF-8 (F), S100A8 (G) and S100A9 (G) in BM cells treated with YCP for 24 h. The values represent the mean±SEM, and all data were analyzed with Student's *t*-test. All experiments were repeated independently at least three times. $^*P<0.05$, $^{**}P<0.01$ compared to the corresponding controls.

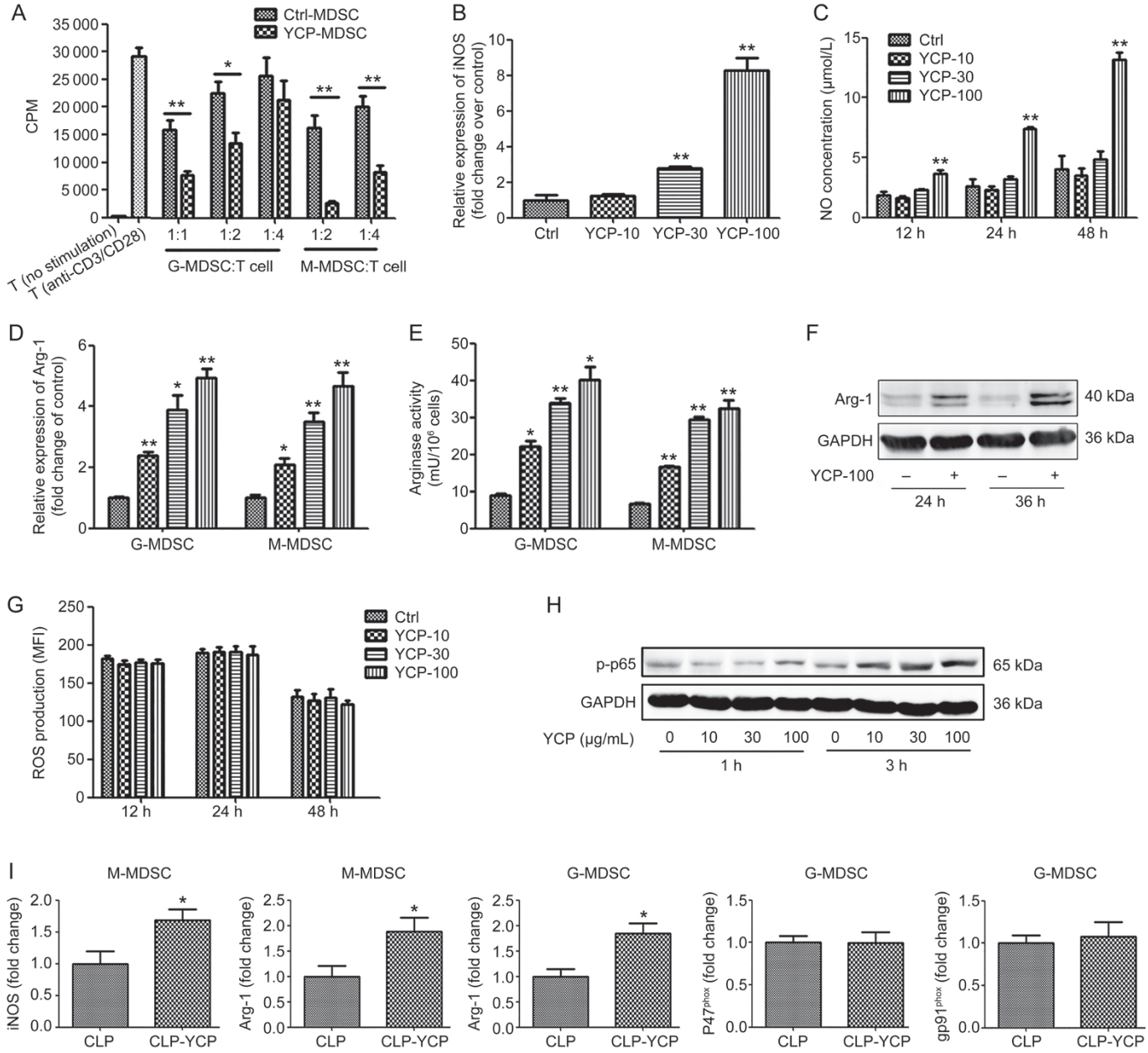

Figure 5. YCP enhances the function of MDSCs, at least partially, through the NF-κB pathway. (A) High purity G-MDSCs and M-MDSCs were obtained from BM-derived MDSCs that were treated with or without 50 μg/mL YCP. For the T cell suppression assay, mouse splenic T cells were co-cultured with purified G-MDSCs or M-MDSCs. All T cells were activated by anti-CD3 and anti-CD28 antibodies. A range of MDSCs:T-cells ratios were used to evaluate T cell suppression. T-cell proliferation was assessed by [^{3}H]thymidine incorporation after 72 h of culture. CPM abbreviation stands for counts per minute. (B, C) Purified M-MDSCs were treated with varying concentrations of YCP. The expression of iNOS was measured by q-PCR at 12 h (B), and the NO production by M-MDSCs was measured with Griess reagent at 12 h, 24 h and 48 h (C). (D) The expression level of Arg-1 in both purified G-MDSCs and M-MDSCs treated with YCP for 24 h were measured by q-PCR. The arginase activity in both purified G-MDSCs and M-MDSCs (E) was measured after the treatment with YCP for 36 h. (F) BM-derived MDSCs were treated with 100 μg/mL YCP for 24 h or 36 h. Arg-1 protein levels were measured by Western blotting. The images are from different parts of the same gel. (G) BM-derived MDSCs were treated with YCP for varying times and identified by anti-Gr1-PE and anti-CD11b-APC. The mean fluorescence in density (MFI) of DCF in Gr1$^+$CD11b$^+$ MDSCs was measured by flow cytometry to detect ROS production. (H) BM-derived MDSCs were treated with YCP for 1 h or 3 h, and the levels of p-p65 were examined by Western blotting. The images are from different parts of the same gel. (I) The MDSCs from the spleens of the septic mice (n=5 per group) treated with or without YCP were harvested 3 d after the CLP operation using an MDSC isolation kit. The expression levels of iNOS, Arg-1, P47^{phox} and gp91^{phox} in these MDSCs were detected by Q-PCR. The values represent the mean±SEM. (A–H) The experiments were repeated independently three times. All data were analyzed with Student's t-test. $^*P$<0.05, $^{**}P$<0.01 compared with the corresponding controls.

the effect of YCP on MDSCs is transmitted through one or both of these receptors, TLR2 and TLR4 knockout mice were used to obtain TLR2$^{-/-}$ or TLR4$^{-/-}$ BM cells. As expected, the absence of TLR4 in the TLR4$^{-/-}$ cells significantly influenced the effect of YCP on MDSC expansion (Figure 6A, 6B). Moreover, the level of IRF-8 in the TLR4$^{-/-}$ BM cells, compared with the normal cells, was significantly decreased after the YCP treatment (Figure 6C). Additionally, the effect of YCP on S100A8 (Figure 6D) and S100A9 (Figure 6E) expression was lost in the TLR4$^{-/-}$, but not the TLR2$^{-/-}$, BM cells. To evaluate the function of MDSCs, BM-derived MDSCs from normal, TLR2$^{-/-}$ and TLR4$^{-/-}$ mice were isolated and treated with 100 μg/mL YCP. The YCP-treated TLR4$^{-/-}$ MDSCs expressed lower levels of iNOS (Figure 6F) and Arg-1 (Figure 6G, 6H), compared with both normal and TLR2$^{-/-}$ MDSCs. Altogether, these results indicate that the TLR4 pathway is necessary for the YCP-mediated inhibition of MDSC expansion and functional enhancement.

Discussion

Sepsis is frequently a fatal condition and is a major cause of death globally[3, 6–8]. The current research direction is to search for effective therapeutic agents for the treatment of sepsis. In the present study, we found that the administration of the α-glucan YCP significantly alleviated multiple organ failure and increased the survival rates of septic mice. Furthermore, we found that YCP not only decreased the production of the pro-inflammatory cytokines IL-6 and TNFα but also regulated the differentiation and functions of MDSCs. The mechanistic study revealed that YCP inhibited the differentiation of MDSCs by blocking the STAT3 pathway and enhanced their functions by activating the NF-κB pathway.

MDSCs isolated from early stage septic mice are not sensitive to stimulation by LPS or IL-6 and produce low levels of Arg-1 and ROS and high levels of TNFα and IL-6 *in vitro*[21, 29]. The adoptive transfer of MDSCs isolated from early stage septic mice into naive mice after CLP increased pro-inflammatory cytokine production and increased early mortality[29]. Thus, these types of cells may be deleterious in controlling sepsis in mice[21, 29]. However, the treatment with YCP significantly altered the state of these MDSCs, simulating a phenotype that is more similar to that observed in late phase MDSCs, including increased iNOS and Arg-1 expression and decreased pro-inflammatory cytokine production *in vivo*. Thus, YCP may protect mice from the early sepsis response by increasing the immunosuppressive function of MDSCs. As the early sepsis response gradually evolves into a sustained immunosuppressed phase, MDSCs and other immunosuppressive cells are dramatically increased[8, 19, 27, 45] and are more sensitive to stimulation by LPS or IL-6[21]. However, the excessive and persistently high proportion of immunosuppressive cells leads to death in late stage sepsis[3, 8, 46]. The YCP treatment decreased the percentage of MDSCs and inflammatory cell infiltration in the injured lung and liver and slightly protected the mice against late sepsis and death.

Previous studies have reported that β-glucans and α-glucans are biologically active when given through different routes of administration, including intraperitoneally, intravenously and orally[11–14, 47–52]. In addition, there was a wide range of differences based on the doses of the different glucans used in these studies, and the variability may be due to the structure of the glucan and the routes of administration. To determine the optimal dose of YCP to use *in vivo*, we tested the effects of 10, 20, and 40 mg/kg YCP administered by intraperitoneal injections on the survival rate of septic mice (data not shown) and found that 20 mg/kg and 40 mg/kg YCP could significantly improve the survival rate. Notably, the effect of 40 mg/kg YCP is not better than that of 20 mg/kg. Hence, the dose of YCP used in this study is 20 mg/kg. Additionally, in this study, both intraperitoneal and intravenous administrations were used to deliver YCP to the septic mice. In addition, we found that YCP administered intraperitoneally improved the survival rate of mice almost equally to that administered intravenously.

STAT3 is arguably the main transcription factor that regulates the expansion of MDSCs[37–39]. Recent studies have suggested that STAT3 may enhance the expansion of MDSCs through the downregulation of IRF8 and the induction of S100A8/S100A9[40, 41]. S100A8/S100A9 complexes play an important role in inflammation[41, 42] and promote lethality in septic shock mouse models[53, 54]. Moreover, IL-6, which is highly elevated in septic mice, can also activate the JAK-STAT3 pathway and promote the expansion of MDSCs[37, 55]. Our results showed that YCP could directly inhibit the phosphorylation of STAT3, induce the expression of IRF8, repress the expression of S100A8 and S100A9 *in vitro* and decrease the level of IL-6 in septic mice *in vivo*. Therefore, YCP inhibited the expansion of MDSCs through a STAT3-dependent pathway. Interestingly, YCP only decreased the percentage of G-MDSCs but not that of M-MDSCs. Albeituni *et al* have reported that the phosphorylation of STAT3 was inhibited in G-MDSCs, but increased in M-MDSCs, following β-glucan stimulation[50]. The decreased STAT3 phosphorylation levels led to MDSC apoptosis[50, 56]. In our study, YCP may also promote the apoptosis of G-MDSCs by inhibiting the STAT3 pathway. However, it is not clear why the accumulation of M-MDSCs was not affected.

We have previously demonstrated that YCP binds to cells via TLR2 and TLR4[15–18]. In this study, our results showed that the absence of TLR4 affected the expansion and function of MDSCs. Although TLR4 is responsible for YCP's modulation of MDSCs, TLR4 is not the only YCP receptor. At high concentrations, the YCP treatment was also able to inhibit MDSC expansion in TLR4$^{-/-}$ BM cells and induce lower levels of iNOS and Arg-1 in TLR4$^{-/-}$ MDSCs. Recently, several groups have reported that β-glucan regulates the differentiation and function of MDSCs through dectin-1, which is a C-type lectin receptor[50–52]. Thus, YCP may activate MDSCs through other receptors that are not toll-like receptors.

In summary, the novel α-glucan YCP significantly protects mice against CLP-induced sepsis. Our findings suggest that the YCP treatment improves both the survival rates and dis-

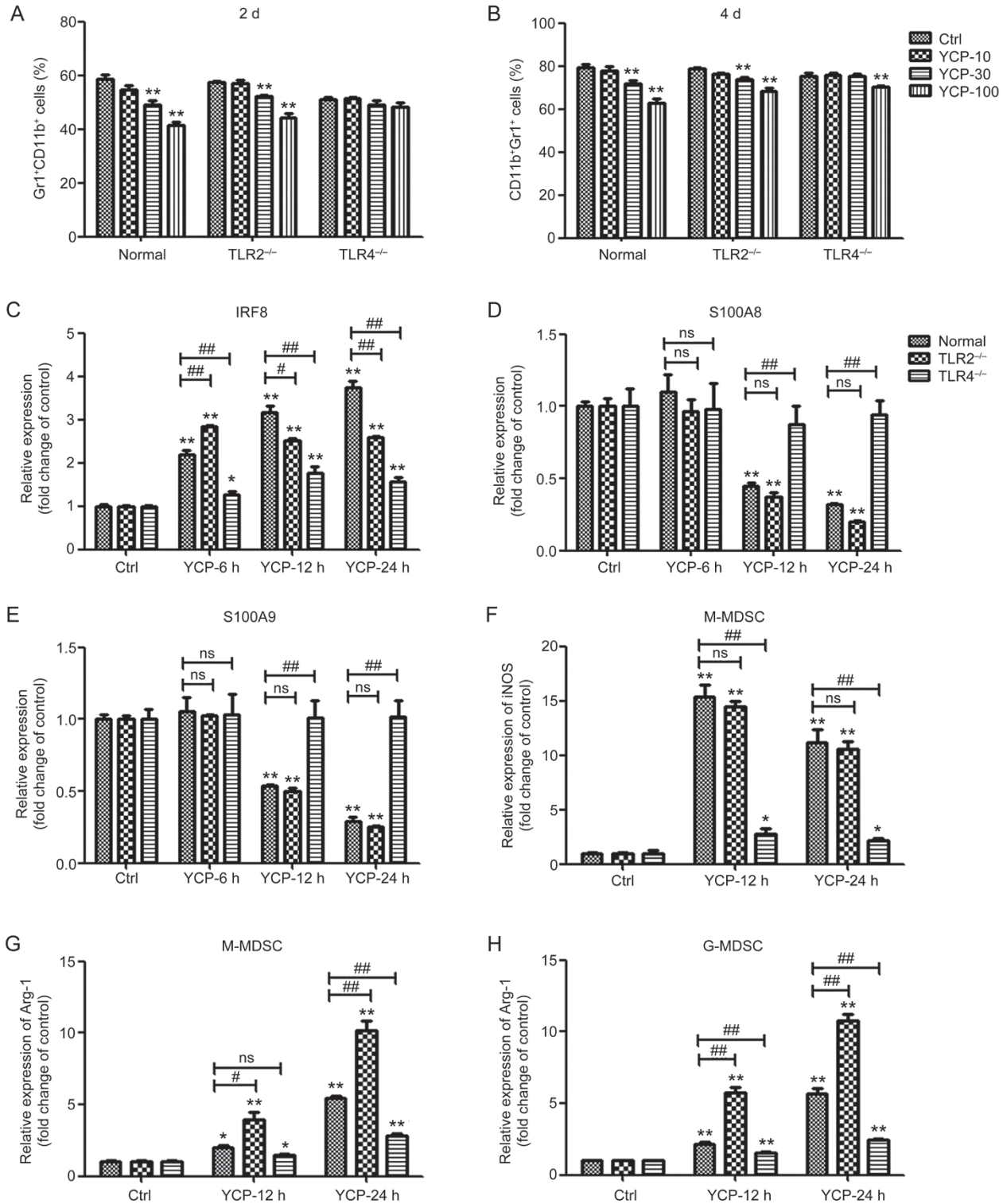

Figure 6. TLR4 on MDSCs acts as the YCP receptor. BM cells from normal, TLR2$^{-/-}$, and TLR4$^{-/-}$ mice were obtained and cultured with 40 ng/mL IL-6 and GM-CSF with or without treatment with YCP. Two (A) or four (B) days later, the cells were collected, and the percentage of Gr1^{+}CD11b^{+} MDSCs was measured by flow cytometry. BM cells of normal, TLR2$^{-/-}$, and TLR4$^{-/-}$ mice were treated with 100 μg/mL YCP for 0 h, 6 h, 12 h or 24 h. The expression levels of IRF-8 (C), S100A8 (D), and S100A9 (E) were measured by q-PCR. BM-derived MDSCs were obtained by culturing BM cells from normal, TLR2$^{-/-}$, and TLR4$^{-/-}$ mice with 40 ng/mL IL-6 and GM-CSF for 4 d and subsequent specific cell subtype isolation to obtain purified G-MDSCs and M-MDSCs. Then, these purified MDSCs were treated with 100 μg/mL YCP for 0 h, 12 h or 24 h. The levels of iNOS (F) in M-MDSCs and Arg-1 in both M-MDSCs (G) and G-MDSCs (H) were measured by q-PCR. The values represent the mean±SEM, and all data were analyzed with Student's *t*-test. All experiments were repeated independently at least three times. $^{*}P<0.05$, $^{**}P<0.01$ compared with the corresponding controls. $^{\#}P<0.05$, $^{\#\#}P<0.01$, TLR2$^{-/-}$ or TLR4$^{-/-}$ versus normal group.

ease symptoms in septic mice through the regulation of MDSC expansion and function. YCP may be a potential therapeutic agent for the treatment of sepsis.

Acknowledgements

This work was supported by a grant from the National Natural Science Foundation of China (Project No 91542113).

Author contribution

Dan LIU, Ya-yi HOU, Xiang-dong GAO, and Wen-bing YAO conceived and directed the project; Dan LIU and Ya-yi HOU designed the experiments; Dan LIU, Ming YOU, Yu-xian SONG, Xiu-jun LI, and Huan DOU carried out all experiments and data analysis; Xiang-dong GAO and Wen-bing YAO purified the α-glucan YCP; Dan LIU wrote the manuscript; and Ya-yi HOU and Guang-feng ZHAO revised the manuscript. All authors reviewed the manuscript.

References

1 Vincent JL, Opal SM, Marshall JC, Tracey KJ. Sepsis definitions: time for change. Lancet 2013; 381: 774–5.
2 Czura CJ. "Merinoff symposium 2010: sepsis" — speaking with one voice. Mol Med 2011; 17: 2–3.
3 Hotchkiss RS, Monneret G, Payen D. Sepsis-induced immunosuppression: from cellular dysfunctions to immunotherapy. Nat Rev Immunol 2013; 13: 862–74.
4 Martin GS, Mannino DM, Eaton S, Moss M. The epidemiology of sepsis in the United States from 1979 through 2000. New Engl J Med 2003; 348: 1546–54.
5 Martin GS, Mannino DM, Moss M. The effect of age on the development and outcome of adult sepsis. Crit Care Med 2006; 34: 15–21.
6 Munford RS, Pugin J. Normal responses to injury prevent systemic inflammation and can be immunosuppressive. Am J Resp Crit Care 2001; 163: 316–21.
7 Xiao W, Mindrinos MN, Seok J, Cuschieri J, Cuenca AG, Gao H, *et al*. A genomic storm in critically injured humans. J Exp Med 2011; 208: 2581–90.
8 Monneret G, Venet F, Pachot A, Lepape A. Monitoring immune dysfunctions in the septic patient: a new skin for the old ceremony. Mol Med 2008; 14: 64–78.
9 Hotchkiss RS, Monneret G, Payen D. Immunosuppression in sepsis: a novel understanding of the disorder and a new therapeutic approach. Lancet Infect Dis 2013; 13: 260–8.
10 Hotchkiss RS, Karl IE. The pathophysiology and treatment of sepsis. N Engl J Med 2003; 348: 138–50.
11 Babayigit H, Kucuk C, Sozuer E, Yazici C, Kose K, Akgun H. Protective effect of beta-glucan on lung injury after cecal ligation and puncture in rats. Intensive Care Med 2005; 31: 865–70.
12 Brown GD, Gordon S. Fungal beta-glucans and mammalian immunity. Immunity 2003; 19: 311–5.
13 Sandvik A, Wang YY, Morton HC, Aasen AO, Wang JE, Johansen FE. Oral and systemic administration of beta-glucan protects against lipopolysaccharide-induced shock and organ injury in rats. Clin Exp Immunol 2007; 148: 168–77.
14 Velazquez EA, Kimura D, Torbati D, Ramachandran C, Totapally BR. Immunological response to (1,4)-alpha-*D*-glucan in the lung and spleen of endotoxin-stimulated juvenile rats. Basic Clin Pharmacol Toxicol 2009; 105: 301–6.
15 Chen S, Ding R, Zhou Y, Zhang X, Zhu R, Gao XD. Immunomodulatory effects of polysaccharide from marine fungus *Phoma herbarum* YS4108 on T cells and dendritic cells. Mediators Inflamm 2014; 2014: 738631.
16 Chen S, Yin DK, Yao WB, Wang YD, Zhang YR, Gao XD. Macrophage receptors of polysaccharide isolated from a marine filamentous fungus *Phoma herbarum* YS4108. Acta Pharmacol Sin 2009; 30: 1008–14.
17 Zhang X, Ding R, Zhou Y, Zhu R, Liu W, Jin L, *et al*. Toll-like receptor 2 and Toll-like receptor 4-dependent activation of B cells by a polysaccharide from marine fungus *Phoma herbarum* YS4108. PLoS One 2013; 8: e60781.
18 Zhu R, Zhang X, Liu W, Zhou Y, Ding R, Yao W, *et al*. Preparation and immunomodulating activities of a library of low-molecular-weight alpha-glucans. Carbohydr Polym 2014; 111: 744–52.
19 Delano MJ, Scumpia PO, Weinstein JS, Coco D, Nagaraj S, Kelly-Scumpia KM, *et al*. MyD88-dependent expansion of an immature GR-1$^+$CD11b$^+$ population induces T cell suppression and Th2 polarization in sepsis. J Exp Med 2007; 204: 1463–74.
20 Makarenkova VP, Bansal V, Matta BM, Perez LA, Ochoa JB. CD11b$^+$/Gr-1$^+$ myeloid suppressor cells cause T cell dysfunction after traumatic stress. J Immunol 2006; 176: 2085–94.
21 Derive M, Bouazza Y, Alauzet C, Gibot S. Myeloid-derived suppressor cells control microbial sepsis. Intensive Care Med 2012; 38: 1040–9.
22 Mathias B, Delmas AL, Ozrazgat-Baslanti T, Vanzant EL, Szpila BE, Mohr AM, *et al*. Human myeloid-derived suppressor cells are associated with chronic immune suppression after severe sepsis/septic shock. Ann Surg 2017; 265: 827–34.
23 McClure C, Brudecki L, Ferguson DA, Yao ZQ, Moorman JP, McCall CE, *et al*. MicroRNA 21 (miR-21) and miR-181b couple with NFI-A to generate myeloid-derived suppressor cells and promote immunosuppression in late sepsis. Infect Immun 2014; 82: 3816–25.
24 Landoni VI, Martire-Greco D, Rodriguez-Rodrigues N, Chiarella P, Schierloh P, Isturiz MA, *et al*. Immature myeloid Gr-1$^+$ CD11b$^+$ cells from lipopolysaccharide-immunosuppressed mice acquire inhibitory activity in the bone marrow and migrate to lymph nodes to exert their suppressive function. Clin Sci (Lond) 2016; 130: 259–71.
25 Knaul JK, Jorg S, Oberbeck-Mueller D, Heinemann E, Scheuermann L, Brinkmann V, *et al*. Lung-residing myeloid-derived suppressors display dual functionality in murine pulmonary tuberculosis. Am J Respir Crit Care Med 2014; 190: 1053–66.
26 Smith AR, Reynolds JM. Editorial: the contribution of myeloid-derived suppression to inflammatory disease. J Leukoc Biol 2014; 96: 361–4.
27 Boomer JS, To K, Chang KC, Takasu O, Osborne DF, Walton AH, *et al*. Immunosuppression in patients who die of sepsis and multiple organ failure. JAMA 2011; 306: 2594–605.
28 Janols H, Bergenfelz C, Allaoui R, Larsson AM, Ryden L, Bjornsson S, *et al*. A high frequency of MDSCs in sepsis patients, with the granulocytic subtype dominating in gram-positive cases. J Leukoc Biol 2014; 96: 685–93.
29 Brudecki L, Ferguson DA, McCall CE, El Gazzar M. Myeloid-derived suppressor cells evolve during sepsis and can enhance or attenuate the systemic inflammatory response. Infect Immun 2012; 80: 2026–34.
30 Sander LE, Sackett SD, Dierssen U, Beraza N, Linke RP, Muller M, *et al*. Hepatic acute-phase proteins control innate immune responses during infection by promoting myeloid-derived suppressor cell function. J Exp Med 2010; 207: 1453–64.
31 Cuenca AG, Delano MJ, Kelly-Scumpia KM, Moreno C, Scumpia PO, Laface DM, *et al*. A paradoxical role for myeloid-derived suppressor cells in sepsis and trauma. Mol Med 2011; 17: 281–92.

32 Ostanin DV, Bhattacharya D. Myeloid-derived suppressor cells in the inflammatory bowel diseases. Inflamm Bowel Dis 2013; 19: 2468–77.
33 Yang XB, Gao XD, Han F, Xu BS, Song YC, Tan RX. Purification, characterization and enzymatic degradation of YCP, a polysaccharide from marine filamentous fungus *Phoma herbarum* YS4108. Biochimie 2005; 87: 747–54.
34 Marigo I, Bosio E, Solito S, Mesa C, Fernandez A, Dolcetti L, *et al*. Tumor-induced tolerance and immune suppression depend on the C/EBPbeta transcription factor. Immunity 2010; 32: 790–802.
35 Rittirsch D, Huber-Lang MS, Flierl MA, Ward PA. Immunodesign of experimental sepsis by cecal ligation and puncture. Nat Protoc 2009; 4: 31–6.
36 Zhao X, Liu L, Liu D, Fan H, Wang Y, Hu Y, *et al*. Progesterone enhances immunoregulatory activity of human mesenchymal stem cells via PGE2 and IL-6. Am J Reprod Immunol 2012; 68: 290–300.
37 Gabrilovich DI, Nagaraj S. Myeloid-derived suppressor cells as regulators of the immune system. Nat Rev Immunol 2009; 9: 162–74.
38 Condamine T, Gabrilovich DI. Molecular mechanisms regulating myeloid-derived suppressor cell differentiation and function. Trends Immunol 2011; 32: 19–25.
39 Nefedova Y, Huang M, Kusmartsev S, Bhattacharya R, Cheng P, Salup R, *et al*. Hyperactivation of STAT3 is involved in abnormal differentiation of dendritic cells in cancer. J Immunol 2004; 172: 464–74.
40 Waight JD, Netherby C, Hensen ML, Miller A, Hu Q, Liu S, *et al*. Myeloid-derived suppressor cell development is regulated by a STAT/IRF-8 axis. J Clin Invest 2013; 123: 4464–78.
41 Cheng P, Corzo CA, Luetteke N, Yu B, Nagaraj S, Bui MM, *et al*. Inhibition of dendritic cell differentiation and accumulation of myeloid-derived suppressor cells in cancer is regulated by S100A9 protein. J Exp Med 2008; 205: 2235–49.
42 Sinha P, Okoro C, Foell D, Freeze HH, Ostrand-Rosenberg S, Srikrishna G. Proinflammatory S100 proteins regulate the accumulation of myeloid-derived suppressor cells. J Immunol 2008; 181: 4666–75.
43 Draghiciu O, Lubbers J, Nijman HW, Daemen T. Myeloid derived suppressor cells-An overview of combat strategies to increase immunotherapy efficacy. Oncoimmunology 2015; 4: e954829.
44 Vlachou K, Mintzas K, Glymenaki M, Ioannou M, Papadaki G, Bertsias GK, *et al*. Elimination of granulocytic myeloid-derived suppressor cells in lupus-prone mice linked to reactive oxygen species-dependent extracellular trap formation. Arthritis Rheumatol 2016; 68: 449–61.
45 Monneret G, Debard AL, Venet F, Bohe J, Hequet O, Bienvenu J, *et al*. Marked elevation of human circulating $CD4^+CD25^+$ regulatory T cells in sepsis-induced immunoparalysis. Crit Care Med 2003; 31: 2068–71.
46 Venet F, Chung CS, Kherouf H, Geeraert A, Malcus C, Poitevin F, *et al*. Increased circulating regulatory T cells ($CD4^+CD25^+CD127^-$) contribute to lymphocyte anergy in septic shock patients. Intensive Care Med 2009; 35: 678–86.
47 Rice PJ, Adams EL, Ozment-Skelton T, Gonzalez AJ, Goldman MP, Lockhart BE, *et al*. Oral delivery and gastrointestinal absorption of soluble glucans stimulate increased resistance to infectious challenge. J Pharmacol Exp Ther 2005; 314: 1079–86.
48 Rice PJ, Lockhart BE, Barker LA, Adams EL, Ensley HE, Williams DL. Pharmacokinetics of fungal (1-3)-beta-*D*-glucans following intravenous administration in rats. Int Immunopharmacol 2004; 4: 1209–15.
49 Sener G, Toklu H, Ercan F, Erkanli G. Protective effect of beta-glucan against oxidative organ injury in a rat model of sepsis. Int Immunopharmacol 2005; 5: 1387–96.
50 Albeituni SH, Ding C, Liu M, Hu X, Luo F, Kloecker G, *et al*. Yeast-derived particulate beta-glucan treatment subverts the suppression of myeloid-derived suppressor cells (MDSC) by inducing polymorphonuclear MDSC apoptosis and monocytic MDSC differentiation to APC in cancer. J Immunol 2016; 196: 2167–80.
51 Tian J, Ma J, Ma K, Guo H, Baidoo SE, Zhang Y, *et al*. beta-Glucan enhances antitumor immune responses by regulating differentiation and function of monocytic myeloid-derived suppressor cells. Eur J Immunol 2013; 43: 1220–30.
52 Tian X, Tian J, Tang X, Rui K, Zhang Y, Ma J, *et al*. Particulate beta-glucan regulates the immunosuppression of granulocytic myeloid-derived suppressor cells by inhibiting NFIA expression. Oncoimmunology 2015; 4: e1038687.
53 Vogl T, Tenbrock K, Ludwig S, Leukert N, Ehrhardt C, van Zoelen MA, *et al*. Mrp8 and Mrp14 are endogenous activators of Toll-like receptor 4, promoting lethal, endotoxin-induced shock. Nat Med 2007; 13: 1042–9.
54 Boyd JH, Kan B, Roberts H, Wang Y, Walley KR. S100A8 and S100A9 mediate endotoxin-induced cardiomyocyte dysfunction via the receptor for advanced glycation end products. Circ Res 2008; 102: 1239–46.
55 Bunt SK, Yang L, Sinha P, Clements VK, Leips J, Ostrand-Rosenberg S. Reduced inflammation in the tumor microenvironment delays the accumulation of myeloid-derived suppressor cells and limits tumor progression. Cancer Res 2007; 67: 10019–26.
56 Nefedova Y, Nagaraj S, Rosenbauer A, Muro-Cacho C, Sebti SM, Gabrilovich DI. Regulation of dendritic cell differentiation and antitumor immune response in cancer by pharmacologic-selective inhibition of the janus-activated kinase 2/signal transducers and activators of transcription 3 pathway. Cancer Res 2005; 65: 9525–35.